Breakup of Ring Beams Carrying Orbital Angular Momentum in Sodium Vapor

Matthew S. Bigelow, Petros Zerom, and Robert W. Boyd

The Institute of Optics, University of Rochester, Rochester, New York 14627, USA

We have observed filamentation due to azimuthal modulational instabilities in spinning ring solitons with orbital angular momentum $m\hbar$ in sodium vapor. We show experimentally that vortex beams with m values of 1, 2, and 3 tend to break into two, four, and six filaments, respectively. Treating the sodium vapor as a Doppler broadened two-level atomic system, we find that we can accurately model the propagation and breakup of these beams with numerical simulations.

PACS numbers: 42.65.Tg, 42.65.Jx

Optical spatial solitons are of great interest because of their potential for applications such as photonics and optical computing [1,2]. Beams that have a ring-shaped intensity pattern and carry orbital angular momentum are of particular interest because of their increased information content and their greater power carrying ability [3]. Such beams have an $e^{im\phi}$ field dependence and carry $m\hbar$ of orbital angular momentum per photon [4]. The entanglement of photons with orbital angular momentum has generated considerable interest [5]. Orbital angular momentum provides an infinite number of quantum states that may be entangled, and thereby may find applications in the field of quantum information such as quantum cryptography.

It is thus of considerable importance to determine how stable ring beams are in propagating through a nonlinear optical material. This problem has been extensively studied analytically and numerically in the literature. However, very little has been done experimentally to study this instability. Rings with $m \leq 2$ have been studied in photorefractive [6] and quadratic materials [7], and atomic vapors [8,9]. We know of no experimental studies of beams with large ($m > 2$) orbital angular momentum numbers. Of particular interest, Minardi *et al.* have shown that it may be possible to use the individual solitons generated in the breakup of vortex beams to perform optical algebraic operations [10].

Although any beam shape is unstable in a pure Kerr medium [11], it is possible to stabilize a single beam by using a material with a saturable Kerr nonlinearity [12]. Ring-shaped solitons are more resistant to whole-beam collapse, but these beams have been shown to have strong azimuthal instabilities in both a saturable Kerr medium and in a material with a competing quadratic $[\chi^{(2)}]$ and cubic $[\chi^{(3)}]$ nonlinearity [13,14]. Specifically, these solitons are most likely to break up into $2m$ filaments that drift away tangentially from the original ring [13].

Nevertheless, it is possible to stabilize these solitons in a competing cubic-quintic $[\chi^{(3)} - \chi^{(5)}]$ medium if the beams are powerful enough [15–18]. It was found by Towers *et al.* that the stability regions of an $m = 1, 2$ soliton take up 9% and 8% of their corresponding exis-

tence regions [16]. It has also been shown that it is possible to stabilize high-power $m = 1, 2$ solitons in a material with a quadratic nonlinearity [19]. In addition, multimode (vector) solitons have also been shown to have improved stability [20,21]. However, in all nonlinear models, it is believed that any $(2 + 1)$D soliton with orbital angular momentum $m \geq 3$ or any $(3 + 1)$D soliton with $m \geq 2$ is not stable [22,23].

In this Letter, we experimentally investigate the stability of beams with orbital angular momentum in a material with a saturable nonlinearity. Specifically, we used a pulsed dye laser and observed the filamentation of solitons with orbital angular momentum values $m = 1, 2$, and 3 in a hot, dense sodium vapor. As predicted by Firth and Skryabin [13], we observed that these beams would break up into two, four, and six filaments, respectively. We compare this result with numerical beam propagation simulations that include an accurate model of the fully saturable nonlinearity in an inhomogeneous two-level system, and show that this model gives excellent agreement with our experimental results. We also observed that these beams show some improved stability at higher powers.

Our experimental setup is shown in Fig. 1. The output of an excimer-pumped dye laser was sent through a spatial filter (SF) to produce a circular TM_{00} beam and was throttled with a half-wave plate (HWP) and polarizing beam splitter (PBS). The pulses had a temporal width (FWHM) of about 15 ns, and were tuned from
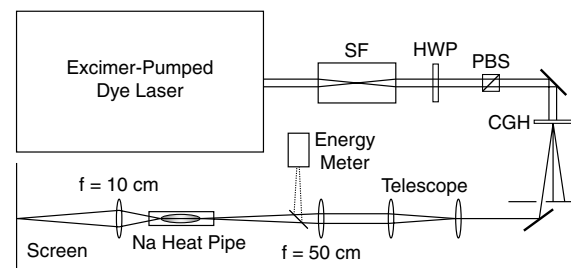

FIG. 1. The experimental setup used to observe filamentation of ring solitons in sodium vapor.

40.6 to 46.7 GHz to the blue side of the D_2 resonance line of sodium. We sent the beam through a bleached computer-generated hologram (CGH) that would produce diffraction orders that are Laguerre-Gauss modes [24,25]. Since the input beam was circular, the generated modes are also circular. The general expression for the field distribution for these modes at the beam waist is given by

$$A_{m,p}(r, \phi) = A_0 \sqrt{\frac{2p!}{\pi w_0^2 (p + |m|)!}} \left(\frac{\sqrt{2}r}{w_0}\right)^{|m|}$$
$$\times L_p^m\left(\frac{2r^2}{w_0^2}\right) e^{-r^2/w_0^2} e^{-im\phi}, \quad (1)$$

where w_0 is the characteristic beam width, and $L_p^m(x)$ is the generalized Laguerre polynomial. The parameters p and m are the radial mode index and the topological charge, respectively. In general, a beam in a given diffraction order would contain a superposition of several modes. However, for our holograms, modes with a radial mode index $p > 0$ were observed to be weak and assumed insignificant to beam propagation dynamics. The conversion efficiency into the first diffraction order was about 5%. One of the diffracted beams was enlarged in a telescope and focused to a 50 μm beam diameter inside the sodium cloud within a heat pipe. A typical value for the number density of the sodium was 8×10^{14} cm^{-3} (depending on cell temperature), and the region of this density was 5 cm long. We added 13 mbar of helium to the heat pipe to act as a buffer gas. Before entering the cell, part of the beam was reflected off a glass slide to monitor the pulse energy. The beam exiting the vapor was imaged onto a screen several meters away where it could be photographed.

Despite the large number of earlier numerical studies of the stability of ring solitons, none of these studies is directly comparable to our system because our input beams are circular Laguerre-Gauss beams and our medium is fully saturable (not cubic-quintic). Therefore, we model the behavior of the atomic vapor in the following manner. Since we were tuned relatively far from resonance ($\Delta > 40$ GHz), we can ignore the hyperfine energy levels and model the sodium vapor as a two-level atom. The density matrix equations of motion for a two-level atom are [26]

$$\dot{\rho}_{ba} = -\left(i\omega_{ba} + \frac{1}{T_2}\right)\rho_{ba} + \frac{i}{\hbar}V_{ba}W, \quad (2a)$$

$$\dot{W} = -\frac{W - W^{(eq)}}{T_1} - \frac{2i}{\hbar}(V_{ba}\rho_{ab} - V_{ab}\rho_{ba}), \quad (2b)$$

where W is the population inversion, $\hbar\omega_{ba}$ is the energy separation between levels a (ground) and b (excited), T_1 is the ground state recovery time, T_2 is the dipole moment dephasing time, and $W^{(eq)}$ is the population inversion of the material in thermal equilibrium. The interaction Hamiltonian in the rotating-wave approximation is given

by $V_{ba} = -\mu_{ba}E(t)e^{-i\omega t}$. To calculate the susceptibility for these equations, it is appropriate to make a steady state approximation [26,27]. With this assumption, we can find an expression for the susceptibility

$$\chi = -\frac{\alpha_0(0)c}{4\pi\omega_{ba}}\frac{\Delta T_2 - i}{1 + \Delta^2 T_2^2 + |E|^2/|E_s^0|^2}, \quad (3)$$

where N is the number density, $\alpha_0(0)$ is the unsaturated resonant absorption coefficient, $\Delta/2\pi$ is the frequency detuning, and E_s^0 is the resonant saturation field strength related to the saturation intensity as $I_s = c/(2\pi)|E_s^0|^2 = N\hbar\omega_{ba}/[2\alpha_0(0)T_1]$. The unsaturated absorption coefficient is $\alpha_0(0) = 4\pi\omega_{ba}N|\mu_{ba}|^2 T_2/(\hbar c)$, and the susceptibility is related to the refractive index as $n = \sqrt{1 + 4\pi\chi} \simeq 1 + 2\pi\chi$. The phase index ($n_0$) and the absorption ($\alpha$) can be found by taking the real and imaginary components of the refractive index given as

$$n_0 = 1 - \frac{\alpha_0(0)c}{2\omega_{ba}}\frac{\Delta T_2}{1 + \Delta^2 T_2^2 + |E|^2/|E_s^0|^2}, \quad (4a)$$

$$\alpha = \alpha_0(0)\frac{1}{1 + \Delta^2 T_2^2 + |E|^2/|E_s^0|^2}. \quad (4b)$$

These expressions for the phase index and absorption for a homogeneously broadened two-level atom given in Eqs. (4) can be extended to an inhomogeneously (Doppler) broadened two-level system [28]. In such a system, the refractive index as a function of laser wavelength (λ) and intensity (I) is given by [29]

$$n_0(\lambda, I) = 1 - \frac{\sqrt{\ln 2}\lambda^3 N}{16\pi^{5/2}T_1\Delta\nu_D}\text{Im}[w(\xi + i\eta)], \quad (5)$$

where N is the number density, $\Delta\nu_D$ is the Doppler linewidth, $\xi = 2\sqrt{\ln 2}(\nu - \nu_{ba})/\Delta\nu_D$ is the normalized detuning frequency, $\eta = \sqrt{\ln 2}/(\pi T_1\Delta\nu_D)\sqrt{1 + I/I_s}$ is power broadened hole size, and $w(z)$ is the complex error function. The absorption can also be found as

$$\alpha(\lambda, I) = -\frac{\eta\lambda^2 N}{8\sqrt{\pi}(1 + I/I_s)}\text{Re}[w(\xi + i\eta)]. \quad (6)$$

It can be shown that by taking the asymptotic form for large z of the complex error function $w(z) \approx i/\sqrt{\pi}z$, Eqs. (5) and (6) reduce to Eqs. (4) [28].

To model our experimental results, we use the propagation equation,

$$\frac{\partial A(x, y, z)}{\partial z} = \frac{i}{2k}\nabla_\perp^2 A(x, y, z) + (-\alpha + ik\Delta n)A(x, y, z), \quad (7)$$

where k is the wave number, Δn is the change in refractive index defined as $\Delta n = n_0(\lambda, I) - n_0(\lambda, 0)$, and $A(x, y, z)$ is the complex amplitude of the electric field $E(x, y, z, t) = A(x, y, z)e^{i(kz - \omega t)}$. We solved Eq. (7) using a standard split-step step fast Fourier transform routine with the input beam profile described in Eq. (1). The parameters
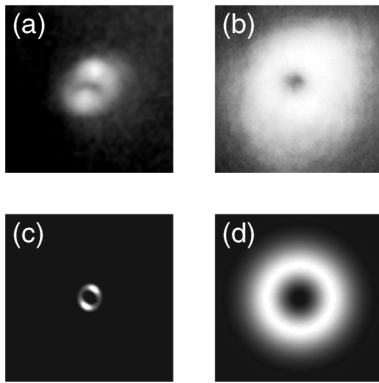
FIG. 2. The experimental output (a) for an $m = 1$ beam with a pulse energy of 76 nJ breaking into two filaments at a wavelength of 588.950 nm, and (b) tuned far from resonance. In (c) and (d) we show the equivalent results from our computer simulations with parameters corresponding to our experiment and a random 1.5% amplitude noise added to the input beam.

for $\alpha(x, y)$ and $n(x, y)$ were found at each step from the measured values from the experiment using Eqs. (5) and (6). In addition, a small amount of random amplitude noise was added to the input beam [30].

Our results for an $A_{1,0}$ beam are shown in Fig. 2. The laser was tuned 40.6 GHz to the blue side of resonance. Because the nonlinearity is large, even at a relatively low input energy (76 nJ), we see that the beam broke up into two filaments [Fig. 2(a)]. For all our results, we found that the patterns generated are quite repeatable provided that the beam quality is good. As mentioned above, we put no intentional perturbation on the beam, and made it as circular as possible. The patterns did not appear to be affected by the orientation of the hologram. Since they did not change from shot to shot, we conclude that the patterns were seeded by imperfections in our system (e.g., dust on lenses and mirrors). We observed these beams breaking up into two spots over a range of pulse energies from 65 to 710 nJ. We show in Fig. 2(b) the same beam tuned far from resonance (nonlinearity off). Figures 2(c) and 2(d) show the output beam from our numerical simulations with and without the nonlinearity ($\Delta n = 0$). A random 1.5% amplitude noise has been added to the input beam.

As expected, the $m = 2$ beam was found to break up into four spots as shown in Fig. 3(a). For this experiment, the laser was tuned 46.7 GHz to the blue side of the D_2 resonance line, and the pulse energy was 234 nJ. The $m = 2$ beam was seen to break into four spots over a pulse energy range of 200 nJ to 1.3 μJ. We also observed that, at higher power, the $m = 2$ beam would break up into five or more spots. It can be seen in Fig. 3(b) that the input beam created by the computer-generated hologram was not a perfect $A_{2,0}$ beam. It had several extra rings around it indicating that it contained higher radial modes. These higher modes do not appear to be stable and appear as noise around the center $A_{2,0}$ beam in Fig. 3(a). Again we
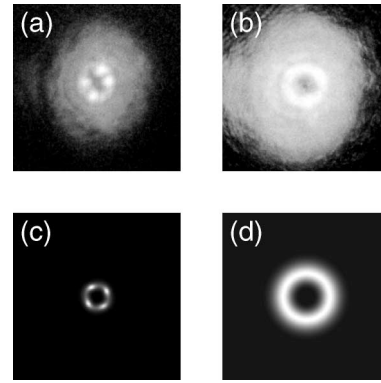

FIG. 3. The experimental output (a) for an $m = 2$ beam with a pulse energy of 234 nJ breaking into four filaments at a wavelength of 588.943 nm, and (b) tuned far from resonance. In (c) and (d) we show the equivalent results from our computer simulations.

see in Figs. 3(c) and 3(d) that the numerical simulations are in excellent agreement with the experiment. As we did in modeling the $m = 1$ case, we added 1.5% random amplitude noise at each point on the input beam to cause the beam to break up.

In Fig. 4, we show the $m = 3$ beam breaking up into six spots. The observed range of six spot filamentation was 350 nJ to 2.5 μJ. The input pulse energy in Fig. 4(a) was 359 nJ, and the laser detuning was again 46.7 GHz. As before, we did not add any intentional perturbation to the beam. While aligning the system, we occasionally saw the beam break up into five or seven spots caused by the seeding of these azimuthal frequencies due to poor beam quality. Poor beam quality can be caused by either misalignment of optics or light scattering off dust on optical surfaces. As we saw in the $m = 2$ beam, the computer-generated $A_{3,0}$ was not perfect and had some higher-order radial modes. For the numerical simulations in Figs. 4(c) and 4(d), we added 1.0% random amplitude noise at each point.
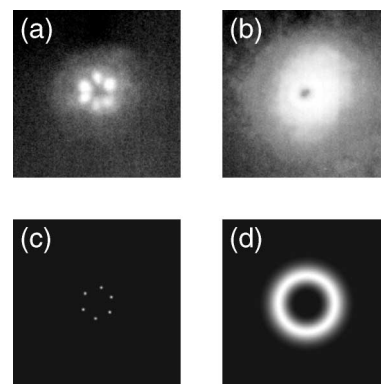

FIG. 4. The experimental output (a) for an $m = 3$ beam with a pulse energy of 359 nJ breaking into six filaments at a wavelength of 588.943 nm, and (b) tuned far from resonance. In (c) and (d) we show the equivalent results from our simulations.
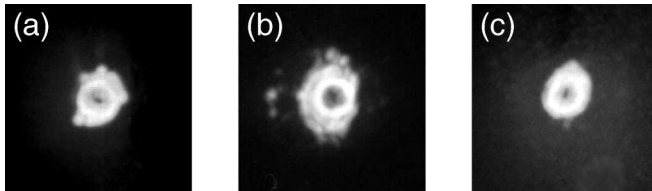
FIG. 5. The beam profile at the output of the sodium cell at higher powers than those used in Figs. 2–4. The tendency of the beam to break into filaments is largely suppressed. (a) $m = 1$ at 9.1 μJ; (b) $m = 2$ at 24.1 μJ; (c) $m = 3$ at 6.63 μJ.

We also experimentally observed the propagation of these beams at higher power. We found that when we increased the power of the beams that they would no longer break up (Fig. 5). The noise seen around the beams in Fig. 5 is the filamentation of the higher-order radial modes. We believe that the observed stability of the $A_{m,0}$ beams is caused by the beam almost completely saturating the nonlinearity, and thereby suppressing the filamentation.

While we made every effort to have perfectly circular input beams, we found that even a small amount of beam ellipticity caused the beam to break into two filaments. Tikhonenko et al. [9] previously observed that an elliptical $m = 2$ beam will break into two spots. However, as expected theoretically [13], we found that an $m = 3$ beam is less susceptible than an $m = 2$ beam to this type of perturbation.

In conclusion, we have experimentally observed that ring beams in a fully saturable nonlinear material that have orbital angular momentum m tend to break up into $2m$ nonrotating spots. Our observation of rings occasionally breaking up into something besides $2m$ beams is consistent with the predictions of Firth and Skryabin [13] since they show that perturbations with the different azimuthal frequencies will grow if seeded, but just not as fast. We compare our experimental results with the propagation of randomly perturbed Laguerre-Gauss beams propagating in a two-level inhomogeneously broadened system, and show that it has excellent agreement with our observations. We have also observed that the beams become considerably more stable at high laser powers, which could prove important for various applications.

[1] G. I. Stegeman and M. Segev, Science **286**, 1518 (1999).
[2] R. McLeod, K. Wagner, and S. Blair, Phys. Rev. A **52**, 3254 (1995).
[3] V. I. Kruglove, Yu. A. Logvin, and V. M. Volkov, J. Mod. Opt. **39**, 2277 (1992).
[4] G. A. Swartzlander, Jr. and C. T. Law, Phys. Rev. Lett. **69**, 2503 (1992); L. Allen et al., Phys. Rev. A **45**, 8185 (1992).
[5] A. Mair et al., Nature (London) **412**, 313 (2001); A. Vaziri, G. Weihs, and A. Zeilinger, J. Opt. B Quantum Semiclassical Opt. **4**, S47 (2002); J. Leach et al., Phys. Rev. Lett. **88**, 257901 (2002).
[6] W. Krolikowski et al., Phys. Rev. Lett. **85**, 1424 (2000).
[7] D. V. Petrov et al., Opt. Lett. **23**, 1444 (1998).
[8] V. Tikhonenko, J. Christou, and B. Luther-Davies, J. Opt. Soc. Am. B **12**, 2046 (1995).
[9] V. Tikhonenko, J. Christou, and B. Luther-Davies, Phys. Rev. Lett. **76**, 2698 (1996).
[10] S. Minardi et al., Opt. Lett. **26**, 1004 (2001).
[11] See, e.g., L. Bergé, Phys. Rep. **303**, 259 (1998).
[12] Y. Chen, Opt. Lett. **16**, 4 (1991); M. Karlsson, Phys. Rev. A **46**, 2726 (1992); D. N. Christodoulides, T. H. Coskun, and R. I. Joseph, Opt. Lett. **22**, 1080 (1997).
[13] W. J. Firth and D. V. Skryabin, Phys. Rev. Lett. **79**, 2450 (1997).
[14] D. V. Skryabin and W. J. Firth, Phys. Rev. E **58**, 3916 (1998).
[15] M. Quiroga-Teizeiro and H. Michinel, J. Opt. Soc. Am. B **14**, 2004 (1997).
[16] I. Towers et al., Phys. Lett. A **288**, 292 (2001).
[17] B. A. Malomed, L.-C. Crasovan, and D. Mihalache, Physica (Amsterdam) **161D**, 187 (2002).
[18] D. Mihalache et al., Phys. Rev. Lett. **88**, 073902 (2002).
[19] A. V. Buryak, Y. S. Kivshar, and S. Trillo, Opt. Lett. **20**, 1961 (1995); I. Towers et al., Phys. Rev. E **63**, 055601 (2001).
[20] Z. H. Musslimani et al., Phys. Rev. E **63**, 066608 (2001); D. Mihalache et al., J. Opt. A Pure Appl. Opt. **4**, 615 (2002).
[21] M. S. Bigelow, Q.-Han Park, and R. W. Boyd, Phys. Rev. E **66**, 046631 (2002).
[22] D. Mihalache et al., Phys. Rev. E **66**, 016613 (2002).
[23] D. Mihalache et al., Phys. Rev. E **67**, 056608 (2003).
[24] N. R. Heckenberg et al., Opt. Quantum Electron. **24**, S951 (1992); H. He, N. R. Heckenberg, and H. Rubinsztein-Dunlop, J. Mod. Opt. **42**, 217 (1995).
[25] N. Kim, Opt. Commun. **105**, 1 (1994).
[26] See, for instance, R. W. Boyd Nonlinear Optics (Academic, San Diego, 1992).
[27] M. L. Dowell et al., Phys. Rev. A **52**, 3244 (1995).
[28] D. H. Close, Phys. Rev. **153**, 360 (1967).
[29] G. A. Swartzlander, Jr., H. Yin, and A. E. Kaplan, J. Opt. Soc. Am. B **6**, 1317 (1989).
[30] We added ~1% random amplitude noise to the input beam in our simulations to match the apparent noise visible in our experimental input beams. We did not consider quantum fluctuations to be significant in our experiments.